14th International Conference on Applications of Statistics and Probability in Civil Engineering, ICASP14
Dublin, Ireland, July 9-13, 2023

A unified approach for reliability analysis of electro-mechanical components of floating offshore substations

Franck Schoefs
Nantes Université, Ecole Centrale Nantes, CNRS, GeM, UMR 6183, IUML FR 3473, F-4400 Nantes(2), France

Mestapha Oumouni
Nantes Université, Ecole Centrale Nantes, CNRS, GeM, UMR 6183, IUML FR 3473, F-4400 Nantes(2), France

Morteza Ahmadivala
France Energies Marines, 29280 Plouzané, France

Neil Luxcey
France Energies Marines, 29280 Plouzané, France

Patrick Guerin
Nantes Université, Ecole Centrale Nantes, CNRS, GeM, UMR 6183, IUML FR 3473, F-4400 Nantes(2), France

ABSTRACT:

By 2050, offshore wind power is expected to become the leading energy source, necessitating the installation of deep-sea turbines and Floating Offshore Sub-Stations (FOSS) for energy transport. However, the FOSS technology is not yet fully developed, and reliability is a significant challenge for the mechanical and electrical subsystems each with distinct approaches to reliability assessment. Consequently, this paper aims to present a unified approach for evaluating the reliability of both the electrical and mechanical components of the FOSS. The resulting methodology can be used to perform a reliability analysis of the FOSS. To demonstrate this, the methodology is applied to a case study situated on the French coasts of the Mediterranean Sea. The study assesses the impact of various mooring and substation designs on system reliability.

1. INTRODUCTION

By 2050, offshore wind energy is predicted to become the primary source of energy, with a six-fold increase in the offshore wind annual market by 2030 and a ten-fold increase by 2050 (IEA Paris, 2019; IRENA, 2019). However, the identification of new sites with significant wind resources is crucial, particularly for deep water depths exceeding 60 meters, where traditional bottom fixed structures are prohibitively expensive. The Floating Offshore Sub-Stations (FOSS) are a promising solution for opening new markets and reducing environmental impact (James et al., 2018).

While floating offshore turbines have been extensively researched, the reliability of offshore substations, a critical component in wind farms, has received less attention (Firestone et al., 2018). Oh et al. (2018) have reviewed different substructures needed to lower construction costs for transitional water depth, and for deeper waters, a Floating Off-

shore Substation (FOSS) with dynamic cables connecting it to both the power generation and grid sides is a relevant solution. However, there is limited understanding of the design rules and life expectancy of FOSS used in renewable energy production (Fukushima Offshore Wind Consortium, 2014).

The FOSS consists of three crucial systems: the export dynamic power cable, the mooring lines, and the electro-technical components. A unified approach for time-variant reliability is proposed here for system reliability analysis in section 2 of the paper. Under certain assumptions, one can use this approach to evaluate the reliability of a system including mechanical and electrical components.

Conducting a comprehensive system reliability assessment for new concepts without existing data is complex, and the paper aims to provide initial results for practical concepts and realistic magnitudes. On that account, Section 3 presents the system architectures of a 250 MW FOSS concept and the main reliability magnitudes for both electro-technical and mechanical components. Section 4 compares the system reliability of FOSS for Mediterranean Sea site using 8 and 12 mooring line architectures and provides a computation and commentary on reliability.

2. Reliability methods for electro-technical and mechanical components

2.1. *Definitions and computation of a failure rate of electro-technical components*

The failure rate, or hazard function, is a key input in reliability analysis of electrical components since it specifies the rate of the system aging. It is defined as the probability per unit time that the device experiences a failure at time $t+\delta t$, given that the device has survived to time t. One can represent the first time of failure with a random variable $\mathbb{T}$ for which $F(t)$ can be used to represent its probability distribution function (i.e., $F(t) = P(\mathbb{T} < t)$) and $f(t)$ can represent its probability density function. The reliability of a component can therefore be defined using Eq. 1 which is equivalent to the probability that the component will not fail during the time interval $(0,t)$.

$$R(t) = 1 - F(t) \tag{1}$$

The usual failure rate, also called hazard function or conditional failure rate, is defined by the following equation at time instant t (Mel, 2017).

$$\begin{aligned} \lambda(t) := \lim_{\delta t \to 0} \frac{P(\mathbb{T} \leq t + \delta t | \mathbb{T} > t)}{\delta t} \\ = -\frac{R'(t)}{R(t)} \end{aligned} \tag{2}$$

where $R'(t)$ is the derivative of the reliability function R with respect to time. Given that $\lambda(t)$ is known in Eq. 2, the reliability function $R(t)$ can be formulated by following equation:

$$R(t) = \exp(-\int_0^t \lambda(r)dr) \tag{3}$$

The Mean Time Between Failure (MTBF) is the expected value of time between two consecutive failures, for a repairable system. The Mean Time to Failure (MTTF) is defined by the arithmetic mean value of the reliability function R, it can be expressed as the expected value of the probability density function $f(.)$. For further definitions such as availability, mean time to repair, etc. in the field of reliability engineering please refer to Sta (2009).

2.2. *Definitions and computation of a failure rate from probability of failure of a mechanical component*

The time-variant structural reliability theory relies on two main indicators, the global failure probability (or safety index) and the out-crossing rate. More information on how to calculate the failure probability can be found in Ahmadivala et al. (2021).

In case of a monotonically decreasing function, cumulative failure probability within time interval $(0,T)$ is equal to the failure probability calculated at time instant T ($P_f(0,T) = P_f(T)$). The annual probability of failure p_f (probability of failure per year) is then computed by the following ratio:

$$p_f = \frac{P_f(T)}{T} \tag{4}$$

where T is the service time of the component. The Vesely failure rate $\lambda_v(t)$ can be used (Amari and

Akers, 2004) to make a connection between the out-crossing rate ν^+ and the failure rate λ as :

$$\lambda(t) = \frac{\nu^+(t)}{1 - P_f(t)} \tag{5}$$

For low instantaneous failure probability, the two quantities are almost equal. Further, in the case of stationary stochastic process and low $P_f(.)$, the failure rate is almost constant such that $\lambda(t) = \nu^+(t)$.

2.3. Annual failure probability and failure rate

Often failure characteristics of structural components are specified with single value, it is the annual failure probability p_f (Eq. 4) which represents the annual mean of analyzed failure events over the life time. As previously mentioned, we consider here statistics from oil and gas industry (FPSO) in view to provide order of magnitudes for these probabilities.

That being the case, by assuming a constant failure rate λ and an exponential distribution of the reliability function, the failure rate λ is computed from the following equation,

$$\lambda(t) = -\frac{\log(1 - p_f T)}{T} \tag{6}$$

for low annual failure probabilities and not large life time T, the failure rate and annual failure probability are almost equal $\lambda \approx p_f$. It should be noted that, the constant failure rate assumption cannot be realistic for some mechanical components.

The cumulative probability density function $P_f(t)$ of a mechanical failure is extrapolated from p_f by affine transformation $P_f(t) = p_f t$ for each $t \leq 1/p_f$. Furthermore, the out-crossing rate ν^+ can be obtained by the derivative of $P_f(t)$.

$$\nu^+(t) = \begin{cases} p_f & t \leq \frac{1}{p_f} \\ 0 & t > \frac{1}{p_f} \end{cases} \tag{7}$$

Thus, by combining Eq.s 7 and 5, the failure rate λ has an increasing behavior and is given by the Eq. 8.

$$\lambda(t) = \begin{cases} \frac{p_f}{1 - p_f t} & t \leq \frac{1}{p_f} \\ \infty & t > \frac{1}{p_f} \end{cases} \tag{8}$$

Naturally, it is important to model the out-crossing rate with a non-constant function of time. Further, this parameter decreases to zeros for large time. Thus, the following out-crossing rate model is introduced.

$$\nu^+(t) = a_1 t^{b_1} e^{-a_2 t^{b_2}} \tag{9}$$

where a_1, a_2, b_1, and b_2 are non-positive real numbers. Further, by combining the Eq. 7 with (5, 3), one writes the following differential equation,

$$\lambda(t) e^{-\int_0^t \lambda(r) dr} = -\frac{d}{dt}(e^{-\int_0^t \lambda(r) dr}) = -a_1 t^{b_1} e^{-a_2 t^{b_2}} \tag{10}$$

The goal is to estimate the failure rate λ from the annual probability p_f. However, Eq. 10 contains several unknown coefficients a_1, a_2, b_1, and b_2. It requires several approximations of the failure probability p_f from the linear interpolation $p_f t$ to get an approximation of the failure rate λ.

Usually, the failure rate of the mechanical components is an increasing function of time. Therefore, considering a power failure rate model λ (which increases similar to the Weibull model) allows to get an analytic solution from only two interpolations of the failure probability $P_f(t = 1)$ and $P_f(t = T)$ where T is the lifetime of the component. To get such analytic solution, we consider the following link between the coefficients a_1, a_2, b_1, and b_2 such that:

$$a_1 = a_2(b_1 + 1) \; and \; b_1 + 1 = b_2 \tag{11}$$

Thus, we use estimate $p_f \approx P_f(1) = 1 - e^{-\int_0^1 \lambda(r) dr}$ and asymptotic estimate of $P_f(T)$ to get the following failure rate

$$\lambda(t) = -(b_1 + 1)\log(1 - p_f) t^{b_1} \tag{12}$$

where the parameter b_1 is defined by

$$b_1 = \log\left(\frac{\log(1 - P_f(T))}{\log(1 - p_f)}\right)(\log(T))^{-1} - 1 \tag{13}$$

Note that the comparison of the MTTF computed from the failure rates in Eq.s 5, 8, and 12 allows to conclude that Eq. 12 gives more reasonable result for MTTF. Particularly, when the annual probability p_f is very small.

2.4. Unified time-dependent reliability computation

The reliability of the electrical system of FOSS is naturally computed through the failure rate $\lambda_{elec}(t)$. Eq. 12 provides a formulation to calculate the failure rate $\lambda_{mech}(t)$ of the mechanical components. This helps to unify the reliability calculation of electrical and mechanical components in a system like FOSS. On that account, the failure rate of FOSS can be uniformly computed by:

$$\lambda_{sys} = \lambda_{elec} + \lambda_{mech} \tag{14}$$

It is worthy to mention that the mechanical and electrical systems are assumed to be serially connected.

3. MAIN BLOCKS OF A FOSS

The FOSS is composed of three main blocks of components from the reliability perspective: mooring & anchor system, floating platform & topside structure, and electro-technical sub-system. Under the availability assumption, these components are connected in series.

The electrical components of the FOSS are divided in two functional subsystems: Main power system including MV/HV transformer(s), HV and MV switchgears (GIS); and Auxiliary system which comprises equipment necessary to safely operate within the design operational conditions. The dynamic power cables (umbilical) can be considered as a member on electrical components which is used to collect the power generated by the floating wind farm and to export it to the hub connecting to the static export cable that goes to the distribution center. Figure 1 represents the electrical configuration of the FOSS with a capacity of 250 MW.

The mechanical part of the FOSS involves the topside structure and the floating support which consists of the floating platform and the mooring system. We only consider the mooring system's reliability assessment within the mechanical components' reliability analyses since the other parts are highly reliable. The substation is designed to be moored from the four corners of the floater by catenary mooring lines. In order to provide redundancy in case of the failure of a line, two configurations will be considered: 4x2 lines and 4x3 lines, see Figure 2.

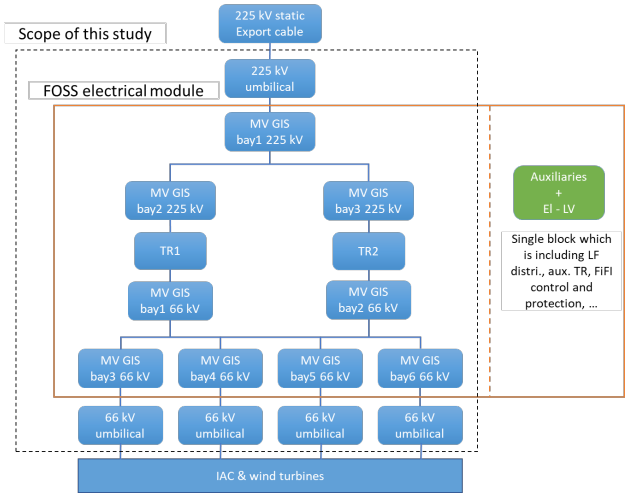

Figure 1: 250 MW, one module, two transformer per module

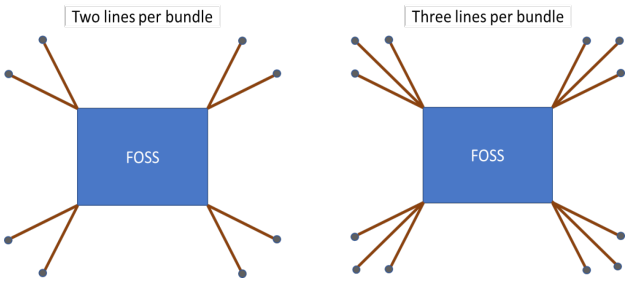

Figure 2: FOSS mooring systems

3.1. Values of component failure rates considered for the electro-technical components

Table 1 provides the required information for the components of the main power system. Preparing such information is straightforward using the feedbacks and statistical information collected by the owners. It should be mentioned that the MTTF is provided according to the minor failures, and

Table 1: MTTF, MTTR, and failure rate of main electrical components

Component	MTTF (years)	MTTR (days)	Failure rate
GIS 66	50	21	0.002
GIS 225	50	21	0.002
Transformer	200	60	0.005
Umb 66	15-40	-	0.025-0.067
Umb 225	15-40	-	0.025-0.067

MTTR is provided according to major repairs. This leads to a conservative estimation of reliability and availability levels of the system. Moreover, the information about the MTTR and MTTF of the umbilical cable is provided according to the experts' opinion.

3.2. Values of component failure rates considered for the mechanical components

Due to the importance of the FOSS in the energy production network, producers prefer mooring systems with the redundancy , i.e., 2 or 3 lines, per anchoring point. This redundancy can be represented by a parallel system. The reliability evaluation approach here relies on the feedback of past failures of mooring lines in a mature industry (offshore oil & gas industry) Ma2 (2013) on which the annual probability of failures p_{rex} of similar but larger systems is available. For reliability analysis, the first objective is to get unknown parameters (in intact and damaged conditions) by knowing p_{rex}. This can be done using a simple limit state $(G(R,F) = R - F$ where R :resistance and F : loading) that includes all the failure cases.

Intact condition: The failure rate of the mooring lines can be obtained using Eq. 12. However, one needs to calculate the values of p_f and $P_f(T)$. For that reason, the loads on mooring lines and their resistance are modelled with random variables without dimension. The events $\{R \leq F_1\}$ and $\{R \leq F_2\}$ obtained from the static equilibrium are nested meaning that the failure of lines will happen in an order since $F_1 \leq F_2$ (see Figure 3). It is assumed that the resultant environmental loading F is perpendicular to the y-axis and acts on one side of the FOSS. Moreover, it is assumed that all lines have the same material properties, dimensions, and the mooring pattern is symmetrical.

The loading F follows a log-normal distribution with a known mean μ_F and unknown standard deviation σ_F. The material strength R also follows a log-normal distribution with a fixed standard deviation σ_R. It is given as a percentage of the maximum breaking load $\mu_R = 1.1$ that does not change during the period of service. Parameter R has a coefficient of variation of $CV_R = 20\%$. The mean value and the variance of load F can be estimated using a sample

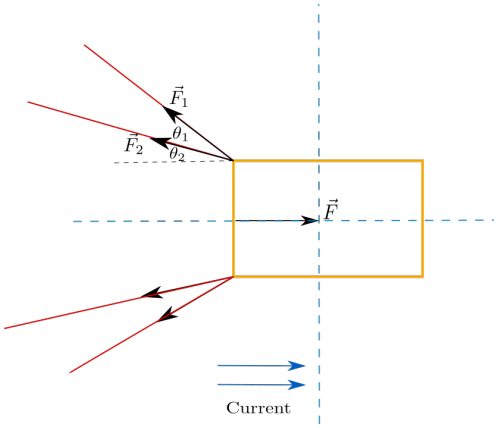

Figure 3: loading conditions on mooring lines (intact condition)

of annual failure probability of one line p_{rex}.

The total failure probability of the system is then approximated using this uncertainty on the environmental load. Knowing the statistics for the environmental loading, static equilibrium can be simply used to evaluate the magnitudes of μ_i, σ_i. The failure probability $p_i = P(R - F_i \leq 0)$ computes the probability that line i breaks $(i = 1,2)$, and it writes:

$$p_i(\sigma) = \int_0^\infty \Phi_R(r)\phi_{F_i}(r)dr \qquad (15)$$

where ϕ_{F_i} is the probability density function (pdf) of the load F_i and Φ_R is the cumulative density function (CDF) of the strength R. Quadrature method is used to estimate the integral 15 in order to obtain an accurate estimation. Further, $p_i(\sigma)$ is a monotonous function of σ, therefore, from a sample value p_{rex} its corresponding value σ is given by inverting the equation $\sigma = p_i^{-1}(p_{rex})$.

Damaged condition: here we consider the case in which one line is damaged. From the nested loading case, l_2 will break first. The remaining load on line 1 is denoted by F_1' where probably $F_1 < F_1'$ (see Figure 4).

It can also be shown that F_1' follows a log-normal distribution with mean $\mu_{F_1'} = \frac{\mu}{2\cos(\theta_1)}$ and standard deviation $\sigma_{F_1'} = \frac{\sigma}{2\cos(\theta_1)}$ where σ is computed from the intact condition case. Similarly, the failure probability of the second line $p_{1|2} = P(R - F_1' \leq 0)$ can be computed with the following integral:

$$p_{1|2}(\sigma) = \int_0^\infty \Phi_R(r)\phi_{F_1'}(r)dr \qquad (16)$$

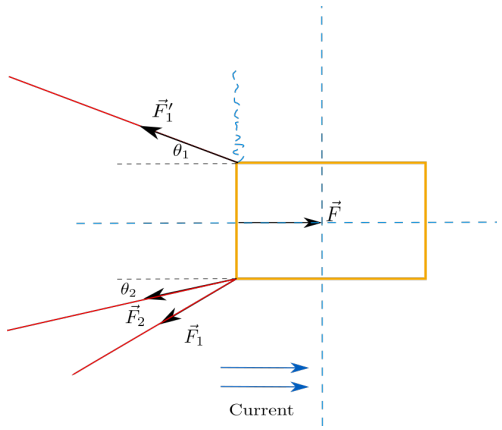

Figure 4: loading conditions on mooring lines (damaged condition)

where $\phi_{F_1'}$ is the pdf of the load F_1'. It should be noted that the random variables F_1' and F_2' have the same coefficient of variation as load F. The probability of the damage of two lines satisfies $P(R \leq F_1; R \leq F_2) = P(R \leq F_1)$ since $F_1 \leq F_2$ (nested load case).

The failure of the system is considered when two lines in the same corner is broken. Therefore, the total failure probability of the system P_{FT} is calculated by:

$$\begin{aligned} P_{FT} &= P((l_1, l_2) \text{ or } (l_1', l_2') \text{ are broken}) \\ &= P(l_1, l_2) + P(l_1', l_2') - P(l_2)P(l_2'|l_2)P(l_1'|l_2, l_2', l_1) \\ &= 2p_2 p_{1|2} - p_2 p_{1|2} p_F \end{aligned} \tag{17}$$

Where by the symmetry and the assumption 2 we obtain $p_2 = P(l_2'|l_2)$, the conditional probability $P(l_1|l_2, l_2') = p_{1|2}$ holds true. The probability $p_F := P(l_1'|l_2, l_2', l_1)$is computed as in Eq. 16 with stress F instead of F_1 or F_2 (it represents the damage probability of line l_1' given the damage of lines l_1, l_2, l_2').

3.3. Installation site

The installation site of the FOSS is "Golfe de Lion" in the Mediterranean Sea, see Figure 5. The estimated water depth of the installation site is 70-100 m. The project partner RTE (Réseau de Transport d'Électricité) provides the required information about the wave height and direction, wind speed and direction, sea current direction, etc. . The provided information about the installation location is used to compute the loading F and design the mooring lines according to the standard using DeepLines software according to DNV (DNV, 2010). The mean values are used for estimation of F_1 and F_2.

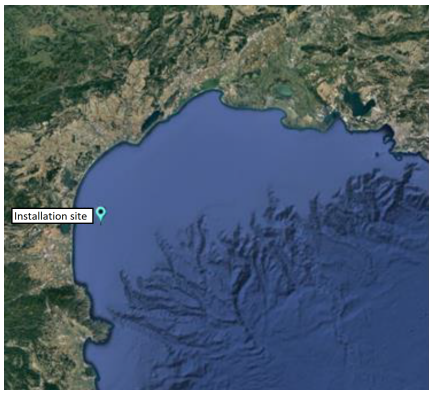

Figure 5: FOSS installation site in the Mediterranean Sea on the coast of France

4. Results and Discussion

4.1. Mooring system time-variant reliability computation

A dynamic approach by DeepLines software is used in order to find the extreme tension in the mooring lines. Table 2 provides the MPM (most probable maximum) effort as calculated for both intact and damage conditions in each scenario. The design effort concerns the maximum tension on the upper lines (l_1, l_2) in the intact and damage conditions. The other lower lines l_1', l_2' are assumed to be loaded nearly like l_1, l_2; whereas, the remaining lines on the other side are subjected to a very weak effort.

We assume nested stresses $F_1 < F_2$ with the same coefficient of variation CV_F. This coefficient is computed by inverting the equation $p_1 = p_{rex}$, where p_1 is the failure probability of the line l_1. The failure probability of the system P_{FT} is estimated by $P_{FT} \approx 2p_1 p_{2|1}$. The probability p_1 is calculated using the lower and upper values $p_{rex} = 0.005,\ 0.02$. From these sample values, we deduce the CV_F to compute the $p_{2|1}$. The material breaking strength R has a coefficient of variation of $CV_R = 20\%$ and the mean μ_R. This is equal to the minimum breaking

Table 2: Case study details

Case	Sub-station	Mooring system	Design tension (MPM)(tons)	Condition
#1	SeeOS1XL 250 MW (2TR185/132MVA)	8 lines, chain, 100mm RS4 Mooring radius: 900 m	497.3 772.8	Intact Damaged
#2	SeeOS1XL 250 MW (2TR185/132MVA)	12 lines, chain, 100mm RS4 Mooring radius: 900 m	316.3 419.2	Intact Damaged

load (MBL) which depend on the diameter of the chain of type $R4s$:

$$\mu_R(R4s) = 0.0304(44 - 0.08d)d^2 \qquad (18)$$

Table 3 provides the failure probabilities with lower and upper estimates of the p_{rex} for two cases in Table 2. Eq.s 12 and 13 are used to calculate the failure rate of the mooring system where $P_F := p_f$, and two asymptotic estimates $P_f(T) = 0.9,\ 0.999$ are respectively used for the lower and upper estimates of P_{FT} of the mooring system at time $T = 60$ years.

Table 3: failure probabilities of mooring lines for considered cases

Cases	#1	#2
μ_R(tons)	1115.977	745.968
CV_F(lower)	0.301	0.344
CV_F(upper)	0.452	0.507
$p_{2\|1}$(lower)	0.140	0.0506
$p_{2\|1}$(upper)	0.204	0.101
P_{FT}(lower)	0.0014	5.06e-04
P_{FT}(upper)	0.00818	0.004

Figure 6 shows the time-dependent curves of the failure rate and reliability of the mooring system with 2 and 3 lines per each corner. It can be easily observed that the mooring system with three mooring lines per corner leads to lower failure rates rather than having only two mooring lines per corner. This is reasonable since the loading on the mooring system is distributed on three mooring lines rather than two lines.

4.2. *Electrical system time variant reliability computation*

In order to simplify the reliability computation of the electrical systems, it can be divided into serial and parallel sub-systems. Figure 7 illustrates the

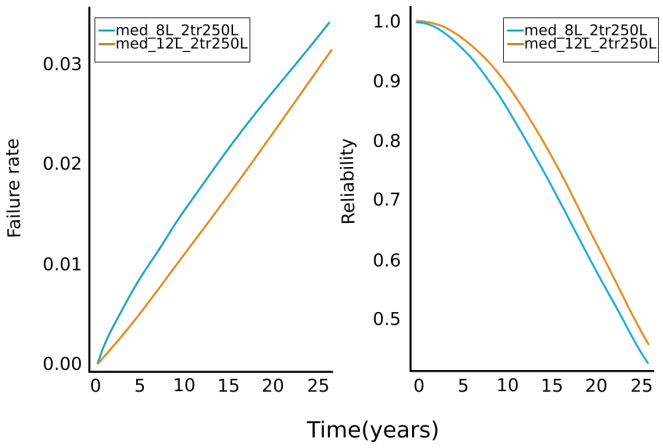

Figure 6: The failure rate and reliability (lower bound) of the mooring system for each scenario

failure rate and reliability curves of the main electrical system. It can be realized that the order of magnitude of the failure rates of the main electrical system is much higher than that for the mooring systems. On that account, the reliability level of the main electrical system decreases faster with time compared to the mooring system.

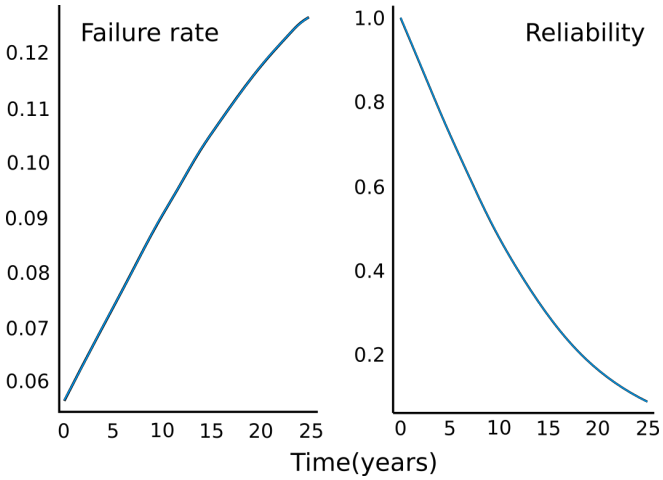

Figure 7: failure rate and reliability curves for the main electrical system

4.3. *FOSS electro-mechanical time variant reliability computation*

Using the proposed unified approach, we can estimate the reliability of the FOSS. Figure 8 demonstrates the time-dependent failure rate and reliability curves of the FOSS. It can be seen that the order of magnitudes of the failure rates and reliability

levels of the FOSS are close to the ones of the main electrical system which means this systems have a significant influence on the reliability of the FOSS. Another important conclusion in the section is that changing the mooring system from 2 lines per corner to 3 lines per corner does not make a big difference on the reliability levels of the FOSS.

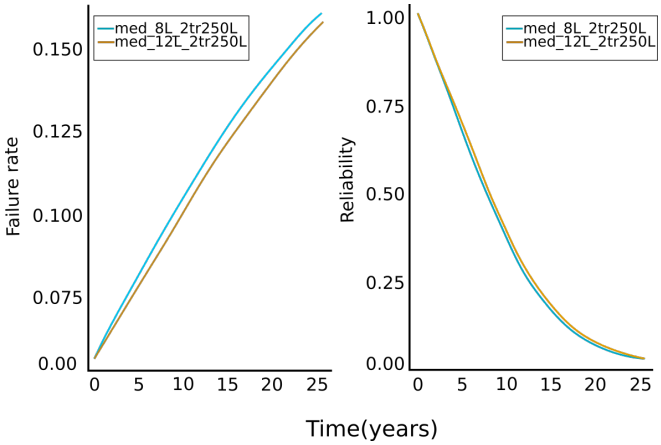

Figure 8: The failure rate and reliability of the FOSS

5. CONCLUSIONS

The main goal of this study is to evaluate the reliability of a new type of offshore structures: floating offshore sub-stations. This requires performing reliability analysis on mechanical and electrical components of the system. A unified approach has been proposed to calculate the failure rate of the FOSS considering both electrical and mechanical subsystems.

The proposed unified approach has been used to evaluate the system's failure rate. The results have shown that the electrical subsystem has a bigger impact on system's reliability. This can be explained by the lower reliability level of the electrical subsystem, and serial connection of electrical and mechanical subsystems in FOSS.

This study has provided the primary results of reliability analysis of an innovative floating offshore substation. Provided results can be enhanced by improving the input information on dynamic cables and mooring lines.

6. REFERENCES

(2009). *Availability and Maintainability in Engineering Design*. Springer London, London, 295–527.

(2013). *A Historical Review on Integrity Issues of Permanent Mooring Systems*.

(2017). *Structural Reliability Assessment*. John Wiley & Sons, Ltd.

Ahmadivala, M., Mattrand, C., Gayton, N., Orcesi, A., and Yalamas, T. (2021). "Ak-sys-t: New time-dependent reliability method based on kriging metamodeling." *ASCE-ASME Journal of Risk and Uncertainty in Engineering Systems, Part A: Civil Engineering*, 7(4), 04021038.

Amari, S. and Akers, J. (2004). "Reliability analysis of large fault trees using the vesely failure rate." *Computer Science, Engineering Annual Symposium Reliability and Maintainability, 2004 - RAMS*.

DNV (2010). "Recommended practice dnv-rp-c205: Environmental conditions and environmental loads." *Technical report*, Det Norske Veritas (October).

Firestone, J., Bates, A. W., and Prefer, A. (2018). "Power transmission: Where the offshore wind energy comes home." *Environmental Innovation and Societal Transitions*, 29, 90–99.

Fukushima Offshore Wind Consortium (2014). "Fukushima floating offshore wind farm demonstration project (fukushima forward)." *Report no.*, Fukushima FORWARD.

IEA Paris (2019). "World energy outlook." *Report no.*, IEA, Paris, <https://www.iea.org/reports/world-energy-outlook-2019>.

IRENA (2019). "Future of wind: Deployment, investment, technology, grid integration and socio-economic aspects." *Report no.*, International Renewable Energy Agency, Abu Dhabi.

James, R., Weng, W., Spradbery, C., Jones, J., Matha, D., Mitzlaff, A., Ahilan, R., Frampton, M., and Lopes, M. (2018). "Floating wind joint industry project - Phase I summary report." *Technical report*, Carbon Trust report (May).

Oh, K.-Y., Nam, W., Ryu, M. S., Kim, J.-Y., and Epureanu, B. I. (2018). "A review of foundations of offshore wind energy convertors: Current status and future perspectives." *Renewable and Sustainable Energy Reviews*, 88, 16–36.